Effects of Coil Locations on Wireless Power Transfer via Magnetic Resonance Coupling

Xinzhi Shi [1], Chang Qi [1], Meiling Qu [1], Shuangli Ye [1], and Gaofeng Wang [2,1]

[1] School of Electronics and Information
Wuhan University, Wuhan 430072, China

[2] Microelectronics CAD Center, School of Electronics and Information
Hangzhou Dianzi University, Hangzhou 310018, China
gaofeng@hdu.edu.cn

***Abstract* ─** The coil locations have strong impacts on efficiency, resonant frequency and bandwidth in the wireless power transfer (WPT) system with four coil resonators, which is a popular configuration for mid-range WPT via magnetic resonance coupling. Herein, effects of coil location parameters, such as the distances between neighboring coils, are investigated by virtue of full-wave electromagnetic solution and validated by measurements. Three operational regions can be defined in terms of the distances between neighboring coils: over coupling, strong coupling and under coupling. It is shown that the distance between the receiving coil and the load coil has significant impact on the power transfer efficiency whereas the distance between the driving coil and the transmitting coil may merely affect the bandwidth and the resonant frequency in the strong coupling regime. In addition, the distance between the transmitting coil and the receiving coil can have strong impact on both the bandwidth and the resonant frequency. Design guidelines for optimal coil locations, by which the highest transfer efficiency or the longest transfer distance can be achieved, are also discussed.

***Index Terms* ─** Magnetic resonance coupling, power transfer distance, wireless power transfer.

I. INTRODUCTION

In recent years, wireless power transfer (WPT) has been drawing a great deal of attention. The WPT technology allows elimination of unsightly, unwieldy and costly power cords and eases anxiety of running out of battery power. The WPT systems have found applications in portable electronic products (e.g., cellular phones, tablet computers), wireless sensor networks (e.g., wireless body sensor networks), implantable medical devices, etc.

Traditionally, the WPT technology has been classified into two types: radio frequency (RF) radiation and inductive coupling in low frequency (LF) bands. RF radiation, which is widely employed for exchanging data and information, can transfer only a small amount of power (e.g., a few milliwatts) because a majority of power is lost into free space [1]. The RF radiation generated by high directional antennas is usually used for WPT [2], such as applications in space solar power station [3]. It can transfer high power over long distances, but requires uninterrupted line-of-sight, which may be harmful to human bodies. On the other hand, the LF-band inductive coupling can transfer power with high efficiency. The LF-band WPT is a mature technology (e.g., it has been widely used in electric toothbrush). Recently, an industry consortium has been formed to standardize this technology for charging mobile devices [4]. However, the LF-band WPT usually transfers power only over a very short range (e.g., a few centimeters).

The recent progress in the WPT technology based on magnetic resonance coupling in high-frequency (HF) bands has opened up a new paradigm for mid-range power transfer [5]. Since then, studies on various aspects of the WPT via magnetic resonance coupling have been conducted [6-19]. The WPT via magnetic resonance coupling has also been extended into various applications [20-25], such as machinery rat [20], underwater robots [21], electric vehicles [22], LED TV [23], medical implants [24], wireless sensor networks [25], etc.

The coil locations have strong impact on efficiency and resonant frequency of the WPT systems using magnetic resonance coupling. So far, however, they are not studied in-depth. In most previous studies, the coil locations of the WPT systems using magnetic resonance coupling are set either without any explanation or simply as equally spaced. There are only a few studies that discussed the coil location effects. In [7], a simple guideline for selecting the optimum repeater locations and numbers were provided. In the case of two repeaters, for example, only two simple rules have been stated: i) the distances of every two coils are equal; ii) the distance between the transmitter and the repeater is equal to the

Submitted On: September 27, 2015
Accepted On: February 26, 2016

distance between the repeater and the receiver. In [10], the relation between resonant frequency and distance was discussed by simply assuming that the total distance is fixed and the equal space is adopted. In [26], the effects of coil inductance and placement have been analyzed.

In this work, effects of the coil locations of the four-coil WPT system via magnetic resonance coupling are studied in-depth by virtue of full-wave electromagnetic solution and validated by measurements. In particular, the dependences of the power transfer efficiency, the resonant frequency and the bandwidth on important location parameters are carefully examined. Some important observations on effects of the coil locations are drawn based on theoretical studies, which are also verified by experiments. Design guidelines for optimal coil locations are presented for the WPT system, to which the highest transfer efficiency or the longest transfer distance can be achieved.

II. SYSTEM MODEL

Consider a four-coil WPT system via magnetic resonance coupling, which is a popular configuration for mid-range WPT via magnetic resonance coupling [5]. This WPT system is composed of four coils: driving coil, transmitting coil, receiving coil and load coil, as shown in Fig. 1. The driving coil (D) is a single loop (i.e., one turn) and connects to the voltage source. The transmitting coil (T) and receiving coil (R) are helix coils. The load coil (L) is also a single loop and connects to the load. The four-coil configuration can reduce the influence of the source and the load, and hence improve the efficiency of the WPT system.

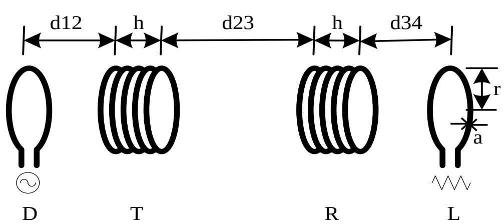

Fig. 1. Schematic of four-coil WPT system.

The four coils are resonant and contactless with each other. The distances (i.e., separations) between the driving and transmitting coils, between the transmitting and receiving coils and between the receiving and load coils are, respectively, denoted as d_{12}, d_{23} and d_{34}. The radius of the four coils, the height of the transmitting and receiving coils and the cross-sectional radius of the conductor coil wires are denoted as r, h and a respectively.

Two types of system models for the WPT system via magnetic resonance coupling are shown in Fig. 2. Panel (a) shows the widely used equivalent circuit model for circuit analysis in the previous published literature, whereas panel (b) illustrates a more accurate model by virtue of full-wave electromagnetic theory.

In panel (a), the driving, transmitting, receiving and load coils are numbered as coils 1, 2, 3 and 4 respectively, M_{ij} (i, j = 1, 2, 3, 4) denotes the mutual inductance between coil i and coil j (and $M_{ij} = M_{ji}$), V_s is ac excitation voltage source with an internal resistance denoted as R_S. The circuit elements C_i, L_i, and R_i (i = 1, 2, 3, 4) represent the parasitic capacitance, self-inductance, and resistance of coil i respectively, R_L is the load resistance connected to coil 4, and the current in coil i is denoted as I_i (i = 1, 2, 3, 4).

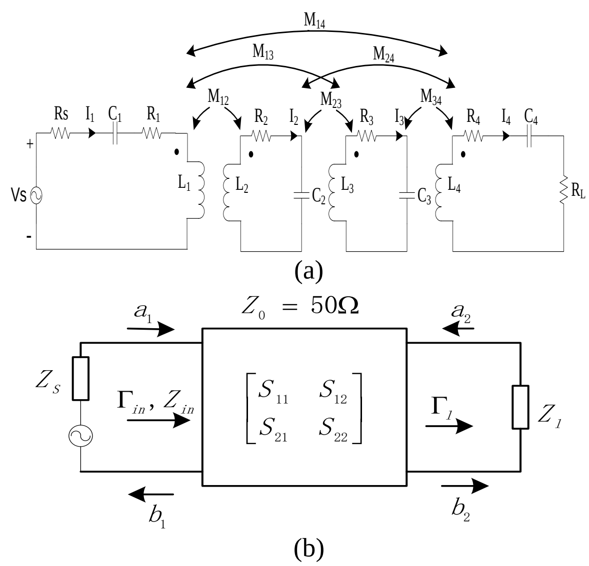

Fig. 2. System models of the WPT system. (a) Equivalent circuit model; (b) two-port S-parameter model.

In panel (b), the WPT system is treated as an integrated (or tightly coupled) unit that is fully characterized as a two-port scattering parameter matrix (i.e., S-parameters) network, in which the transmitting port is denoted as port 1 and the receiving port is denoted as port 2. The S-parameter matrix can be obtained from the full-wave electromagnetic solution. The driving coil is excited by ac excitation voltage source V_s with internal resistance R_S, while the load coil is connected to the load resistance R_L.

Instead of the equivalent circuit model, the more accurate two-port S-parameter model is adopted to study the WPT system by virtue of the full-wave electromagnetic solution. Based on the S-parameters, the power transfer efficiency of the WPT system can be evaluated as:

$$\eta = \frac{P_l}{P_{in}} = \frac{|S_{21}|^2\left(1-|\Gamma_L|^2\right)}{|1-S_{22}\Gamma_L|^2\left(1-|\Gamma_{in}|^2\right)}, \qquad (1)$$

where Γ_L is the reflection coefficient at the load $Z_L = R_L$, and Γ_{in} is the reflection coefficient at port 1. They can be calculated as:

$$\Gamma_L = \frac{Z_L - Z_0}{Z_L + Z_0}, \quad (2)$$

$$\Gamma_{in} = S_{11} + \frac{S_{12}S_{21}\Gamma_L}{1 - S_{22}\Gamma_L}, \quad (3)$$

where S_{11}, S_{21}, S_{12} and S_{22} are the S-parameters, as shown in Fig. 2 (b). If mismatching at the port 1 is omitted, the maximum transfer efficiency can be achieved when the load meets the following matching condition:

$$\Gamma_l = S_{22}^*(f). \quad (4)$$

In the following section, the S-parameters are computed by using the full-wave electromagnetic solution in reference to a characteristic impedance. $Z_0 = 50\,\Omega$

III. EFFECTS OF COIL LOCATIONS

In this section, analysis on coil locations of the WPT system via magnetic resonance coupling, as shown in Fig. 1, is presented by virtue of the full-wave electromagnetic solution. The full-wave electro-magnetic solution is obtained by a commercial full-wave electromagnetic simulation tool, called FEKO. The four coils are made of Cu. The geometrical and physical parameters are listed in Table 1.

Table 1: Parameters of the WPT system

Symbol	Meaning	Value	Unit
r_1	Radius of driving coil	30	cm
r_2	Radius of transmitting coil	30	cm
r_3	Radius of receiving coil	30	cm
r_4	Radius of load coil	30	cm
a	Cross-sectional radius of coil wires	0.3	cm
h	Height of the transmitting coil and the receiving coil	20	cm
N	Number of turns of the transmitting coil and the receiving coil	5.25	turn
R_S	Internal resistance of voltage source	50	ohm
R_L	Load resistance	550	ohm

The distance parameters include d_{12}, d_{23} and d_{34}. The total transfer distance between the driving coil and the load coil is defined as:

$$d = d_{12} + d_{23} + d_{34}. \quad (5)$$

Note that the heights of the transmitting coil and the receiving coil are not included in the total transfer distance.

Electromagnetic simulations are performed by FEKO to study effects of coils locations (i.e., distances between pairs of adjacent coils) in terms of the power transfer efficiency, the resonant frequency and the bandwidth. Note that, in the WPT system via magnetic resonance coupling, the input power has little impact on the power transfer efficiency as theoretically expected since this WPT system is linear and the input power has been factored out from the power transfer efficiency as shown in its definition (1).

A. Effects of variable d_{34} with fixed d_{12} and fixed d_{23}

In this subsection, effects of d_{34} on efficiency of the WPT system via magnetic resonance coupling are studied. It is assumed that d_{34} varies from 5 cm to 60 cm with a step size of 5 cm, whereas d_{12} is fixed at 15 cm and d_{23} is fixed at 150 cm. The efficiency versus d_{34} is plotted in Fig. 3, while the efficiency versus the frequency is depicted in Fig. 4.

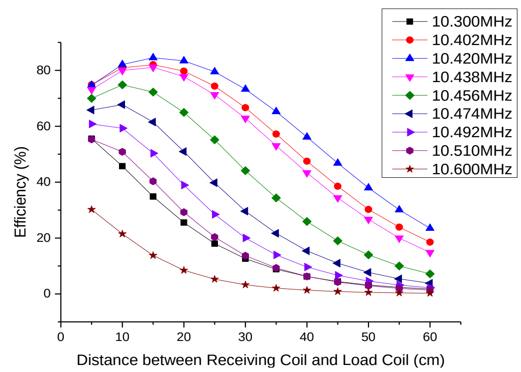

Fig. 3. Efficiency versus d_{34} (with fixed d_{12} and fixed d_{23}).

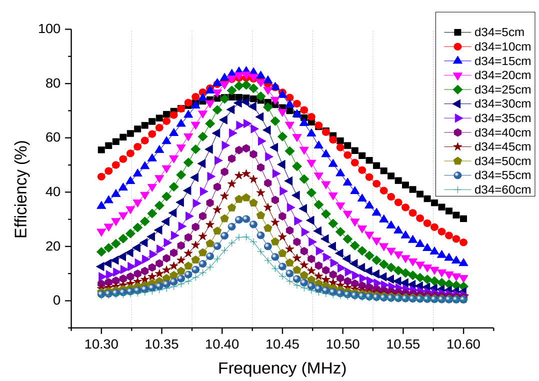

Fig. 4. Efficiency versus frequency (with fixed d_{12} and fixed d_{23}).

From Fig. 3, one can observe that when d_{34} increases from 5 cm to 60 cm, the power transfer efficiency increases at beginning, then becomes saturated, and finally decreases in a downward trend for the frequencies no larger than 10.474 MHz. When d_{34} is shorter than 10 cm, the closer the receiving and load coils are, the lower the efficiency is. When d_{34} is between 10 cm and 20 cm, the efficiency is almost flattened within a small range from 82.07% to 84.51%. When d_{34} is beyond 20 cm, the efficiency diminishes dramatically.

The efficiency is the highest around the frequency of 10.42 MHz regardless the value of d_{34}. When the operating frequency shifts roughly 1.5% from 10.42 MHz (such as 10.300 MHz and 10.600 MHz), the efficiency decreases dramatically as shown in Fig. 3. The highest efficiency can be obtained as 85.51% when d_{34} is 15 cm and the operating frequency is 10.42 MHz.

From Fig. 4, one can observe that when d_{34} is shorter than 10 cm, the bandwidth is wide but the efficiency is not very high. For example, when d_{34} is 5 cm, the bandwidth is 0.174 MHz and the highest efficiency is only 74.97%.

When d_{34} is between 10 cm and 20 cm, the bandwidth becomes narrower, but the highest efficiency is always above 80%. For example, when d_{34} is 10 cm, 15 cm and 20 cm, the bandwidth is 0.144 MHz, 0.114 MHz and 0.090 MHz respectively, whereas the efficiency can be as high as 82.07%, 84.51% and 83.49% respectively.

When d_{34} is longer than 20 cm, the bandwidth is still narrow and the efficiency becomes lower. For example, when d_{34} is 30 cm, the bandwidth is 0.042 MHz and the highest efficiency is 73.24%. When d_{34} is 60 cm, the highest efficiency is now as low as 23.49%.

From Fig. 4, one can see that the resonant frequency is 10.408 MHz when d_{34} is 5 cm. The resonant frequency stays almost constant at 10.42 MHz for all d_{34} from 10 cm to 60 cm.

B. Effects of variable d_{23} with fixed d_{12} and fixed d_{34}

Effects of d_{23} on efficiency of the WPT system via magnetic resonance coupling are studied in this subsection. It is assumed that d_{23} varies from 20 cm to 300 cm with a step size of 20 cm, whereas d_{12} and d_{34} are fixed at 15 cm. The efficiency versus d_{23} is plotted in Fig. 5, while the efficiency versus the frequency is depicted in Fig. 6.

From Fig. 5, one can see that when d_{23} increases from 20 cm to 300 cm, the power transfer efficiency increases at beginning, then becomes saturated, and finally decreases considerably. When d_{23} is shorter than 40 cm, the closer the transmitting and receiving coils are, the lower the efficiency is. When d_{23} is between 40 cm and 120 cm, the efficiency is almost flattened within a small range from 89.69% to 92.23%. When d_{23} is beyond 120 cm, the efficiency diminishes dramatically.

The efficiency is the highest at the frequency of 10.455 MHz for most values of d_{23}. When the operating frequency shifts roughly 1.5% from 10.455 MHz (such as 10.300 MHz and 10.600 MHz), the efficiency decreases dramatically as shown in Fig. 5. The highest efficiency can be obtained as 92.23% when d_{23} is 60 cm and the operating frequency is 10.455 MHz.

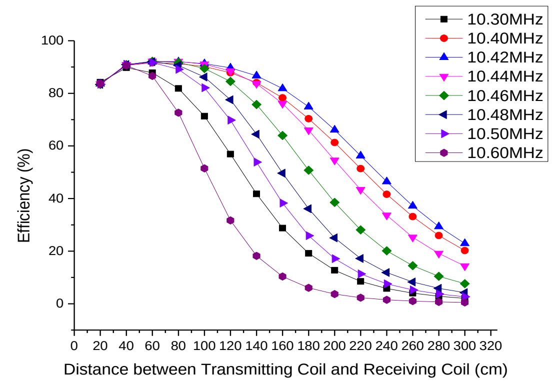

Fig. 5. Efficiency versus d_{23} (with fixed d_{12} and fixed d_{34}).

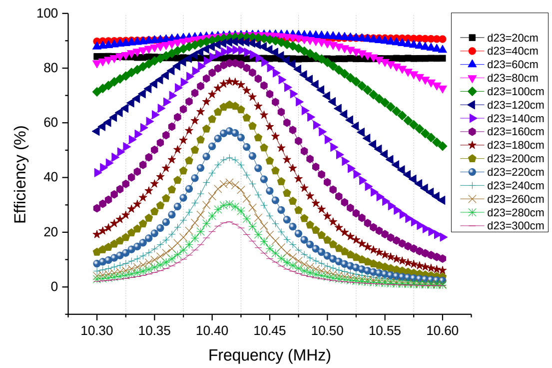

Fig. 6. Efficiency versus frequency (with fixed d_{12} and fixed d_{34}).

From Fig. 6, one can see that when d_{23} is within 40 cm, the bandwidth is very wide but the efficiency still has some room to improve. For example, when d_{23} is 20 cm, the bandwidth is wider than 0.3 MHz while the highest efficiency is 84.28%.

When d_{23} is between 40 cm and 120 cm, the bandwidth becomes narrower, but the highest efficiency is always above 85%. For example, when d_{23} is 80 cm and 120 cm, the bandwidth is 0.2 MHz and 0.065 MHz respectively, whereas the efficiency can be as high as 92.15% and 89.69% respectively.

When d_{23} is longer than 120 cm, the bandwidth is still narrow and the efficiency becomes much lower. For example, when d_{23} is 140 cm, the bandwidth is 0.025 MHz and the highest efficiency is 86.68%. When d_{23} is 300 cm, the highest efficiency is now as low as 23.82%.

From Fig. 6, one can observe that the resonant frequency is 10.31 MHz when d_{23} is 20 cm. The resonant frequency decreases when d_{23} increases from 40 cm to 120 cm. For example, the resonant frequency is 10.50 MHz, 10.43 MHz and 10.42 MHz when d_{23} is 40 cm, 80 cm and 120 cm respectively. The resonant frequency stays almost constant at 10.42 MHz for all d_{23} beyond 120 cm.

By comparing Fig. 5 to Fig. 3, one can see that the efficiency keeps high for a relatively large range of d_{23}.

That is, the distance d_{23} between the transmitting and receiving coils has a wide range of the strong coupling state. Therefore, the distance d_{23} can be used for expanding the total transmission distance.

C. Effects of variable d_{12} with fixed d_{23} and fixed d_{34}

Effects of d_{12} on efficiency of the WPT system via magnetic resonance coupling are studied in this subsection. It is assumed that d_{12} varies from 5 cm to 240 cm, whereas d_{23} is fixed at 150 cm and d_{34} is fixed at 15 cm. The efficiency versus d_{12} is plotted in Fig. 7, while the efficiency versus the frequency is depicted in Fig. 8.

From Fig. 7, one can observe that when d_{12} increases from 5 cm to 240 cm, the power transfer efficiency is stable at beginning and then rapidly decreases. When d_{12} is shorter than 60 cm, the efficiency varies slightly from 84.14% to 84.51%. When d_{12} is beyond 60 cm, the efficiency diminishes dramatically.

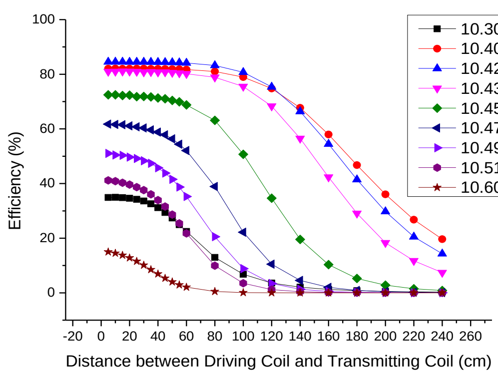

Fig. 7. Efficiency versus d_{12} (with fixed d_{23} and fixed d_{34}).

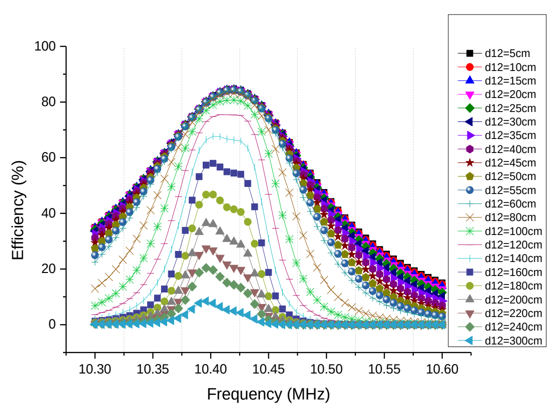

Fig. 8. Efficiency versus frequency (with fixed d_{23} and fixed d_{34}).

The efficiency is the highest at the frequency of 10.42 MHz regardless the value of d_{12}. When the operating frequency shifts roughly 1.5% from 10.42 MHz (such as 10.300 MHz and 10.600 MHz), the efficiency decreases dramatically as shown in Fig. 7. The highest efficiency can be obtained as 84.51% when d_{12} is 15 cm and the operating frequency is 10.42 MHz.

From Fig. 8, one can observe that when d_{12} is within 60 cm, the bandwidth decreases slightly along with increasing d_{12}, but the highest efficiency is nearly constant. For example, when d_{12} is 5 cm and 60 cm, the bandwidth is 0.114 MHz and 0.096 MHz while the highest efficiency is 84.51% and 84.14% respectively.

When d_{12} is longer than 60 cm, the bandwidth becomes narrower and the efficiency becomes much lower. For example, when d_{12} is 140 cm, the bandwidth is 0.042 MHz and the highest efficiency is 67.73%. When d_{12} is 240 cm, the highest efficiency is now down to 20.38%.

From Fig. 8, one can see that the resonant frequency stays almost constant at 10.42 MHz for all d_{12} from 5 cm to 100 cm. The resonant frequency slightly decreases when d_{12} gets longer beyond 100 cm. For example, when d_{12} is 120 cm and 240 cm, the resonant frequency is 10.408 MHz and 10.396 MHz respectively.

By comparing Fig. 7 to Fig. 3, it is found that the distance d_{12} between the driving and transmitting coils has a wide range of the strong coupling state, which is very beneficial for expanding the total transmission distance via increasing d_{12}.

D. Effects under fixed total transfer distance

Location effects on efficiency of the WPT system via magnetic resonance coupling are studied under a fixed total transfer distance d in this subsection. It is assumed that d is fixed at 200 cm, whereas d_{12} and d_{34} are always equal and vary from 10 cm to 70 cm with a step size of 10 cm. Correspondingly, $d_{23} = d - 2d_{12}$ varies from 180 cm to 60 cm with a step size of 20 cm. The efficiency versus d_{12} (i.e., d_{34}) is plotted in Fig. 9, while the efficiency versus the frequency is depicted in Fig. 10.

From Fig. 9, one can observe that when d_{12} and d_{34} increase from 10 cm to 70 cm (i.e., d_{23} decreases from 180 cm to 60 cm), the power transfer efficiency increases at beginning and then decreases. From Fig. 9, one can observe that when d_{12} and d_{34} are shorter than 20 cm (i.e., d_{23} is longer than 160 cm), the closer the driving (receiving) and transmitting (load) coils are, the lower the efficiency is. Frequency splitting occurs when the distance between the driving (receiving) and transmitting (load) coils becomes too small and thus leads to lower efficiency. When d_{12} and d_{34} are longer than 20 cm, the efficiency diminishes dramatically.

The efficiency is the highest at the frequency of 10.42 MHz regardless the values of d_{12}, d_{23} and d_{34}. When the operating frequency shifts roughly 1.5% from 10.42 MHz (such as 10.300 MHz and 10.600 MHz), the efficiency decreases dramatically as shown in Fig. 9. The highest efficiency can be obtained as 81.68% when d_{12} and d_{34} are 20 cm (i.e., d_{23} is 160 cm) and the operating frequency is at the resonant frequency (i.e., 10.42 MHz).

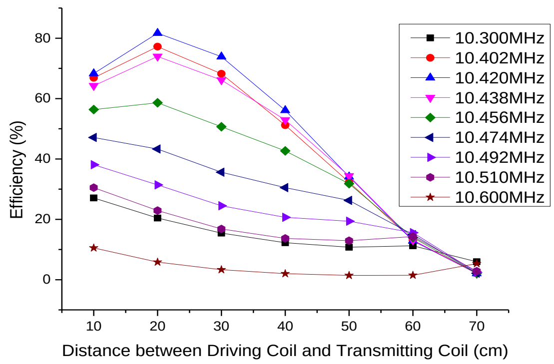

Fig. 9. Efficiency versus d_{12} (with d_{23} = d -2d_{12}, d_{34} = $d_{12}$and fixed d).

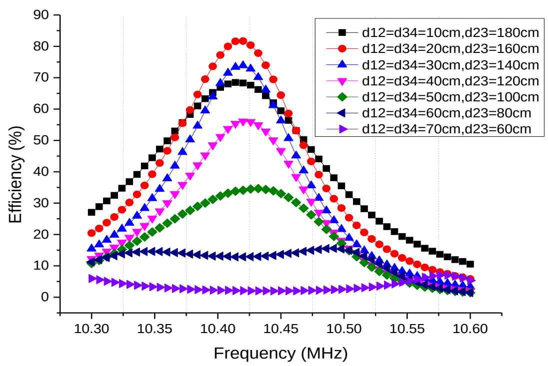

Fig. 10. Efficiency versus frequency (with d_{23} = d -2d_{12}, d_{34} = $d_{12}$and fixed d).

From Fig. 10, one can observe that when d_{12} and d_{34} are within 10 cm (i.e., d_{23} is beyond 180 cm), the bandwidth is relatively wide although the efficiency is not very high. For example, when d_{12} and d_{34} are 10 cm (i.e., d_{23} is 180 cm), the bandwidth is 0.06 MHz while the highest efficiency is only 68.48%.

When d_{12} and d_{34} increase from 20 cm to 50 cm (i.e., d_{23} decreases from 160 cm to 100 cm), the bandwidth becomes narrower and the efficiency becomes lower. When d_{12} and d_{34} are longer than 60 cm (i.e., d_{23} is shorter than 80 cm), the frequency splitting occurs and the efficiency is very low.

E. Discussions

Based on the preceding subsections, it is evident that the locations of four coils have strong impact on the efficiency, the resonant frequency and the bandwidth of the WPT system via magnetic resonance coupling. Some interesting observations can be drawn as follows.

The operation of the WPT system via magnetic resonance coupling can be divided into three regions in terms of the distance between each pair of two coils: over coupling, strong coupling and under coupling. The system is in the over coupling state if two coils (e.g., driving and transmitting coils, transmitting and receiving coils, or receiving and load coils) are too close to each other. When the system is in the over coupling state, the power transfer efficiency is usually low due to frequency splitting. The closer the two coils are, the lower the efficiency is. In addition, the resonant frequency may shift to a lower frequency when the system is in over coupling.

The system is in the under coupling state if two coils are too far away. When the system is in the under coupling state, the power transfer efficiency decreases along with increasing distance due to weakened coupling.

The system is in the strong coupling state if two coils are at a suitable distance. The power transfer efficiency achieves the highest and keeps almost constant regardless the distance variation within a certain range. However, the efficiency can decrease dramatically if the operating frequency deviates too far from the resonance frequency.

By adjusting locations of four coils, the WPT system via magnetic resonance coupling can be made to operate in different states. The system operates in the strong coupling state if the following conditions are satisfied: $\frac{2}{3}r \le d_{12} \le \frac{5}{3}r$, $\frac{4}{3}r \le d_{23} \le 4r$, and $\frac{1}{3}r \le d_{34} \le \frac{2}{3}r$ (where r is the coil radius).

The distances d_{12}, d_{23} and d_{34} have different impacts on the efficiency of the WPT system via magnetic resonance coupling. The distance d_{34} between the receiving and load coils has more significant impact on the efficiency than the distance d_{12} between the driving and transmitting coils. This is because the load coil is connected to the load. The variation of d_{34} changes the load impedance and therefore affects the power transfer efficiency.

In the strong coupling state, the bandwidth is usually broadened and the resonant frequency shifts to a lower frequency. Interestingly, the distance d_{12} between the driving and transmitting coils has a wide range of the strong coupling state. Consequentially, the efficiency does not change much with the variation of d_{12} in the strong coupling state (as shown in Fig. 7), which is very beneficial for expanding the total transmission distance via increasing d_{12}.

The distance d_{23} between the transmitting and receiving coils has a wide range of the strong coupling state too. However, it has strong impact on the bandwidth and the resonant frequency of the WPT system via magnetic resonance coupling. Therefore, one may expect some small adjustment on the resonant frequency when the distance d_{23} is used for expanding the total transmission distance yet maintaining high efficiency.

There exists an optimal set of coil locations for the WPT system via magnetic resonance coupling under the assumption of a fixed total transfer distance. When the highest efficiency is the objective, the locations of four coils should be assigned according to the following guideline: $d_{12} \approx d_{34} \approx 0.5r$ and $d_{23} \approx 2r$ (where r is the coil radius).

If the longest transfer distance is the objective under a fixed efficiency, one should hold d_{34} at the upper limit of the strong coupling region (e.g., $d_{34} \approx \frac{2}{3}r$), and then stretch d_{12} and d_{23} as much as possible over their strong coupling regions (e.g., d_{12} and d_{23} can be, respectively, as large as two and four times of the coil radius) until the efficiency hits the targeted value.

Note that, although the results obtained for the specific coil radii 30 cm, the basic concept of this work is useful and can be a good guide for other radii. For a larger system, such as a "domino" system, which has coils more than four, similar analysis can be conducted and similar design guidelines are expected. The relay coils can be inserted between the transmitting coil and the receiving coil. The effects of these coil locations on WPT systems are similar to the effect of d_{23}.

IV. PRACTICAL VERIFICATION

Experiments have been carried out to verify the theoretical studies by using a four coil WPT system via magnetic resonance coupling, as shown in Fig. 11. The geometrical and physical parameters of the system are the same as those listed in Table 1. Compensating capacitors are added to the driving, transmitting, receiving and load coils to make them resonant at the frequency of 10.42 MHz. The related parameters are listed in Table 2.

Fig. 11. Photograph of the WPT system for experiments.

Table 2: Parameters of four coils

Parameters	Value
Inductance of driving coil (μH)	1.7661
Capacitance of driving coil (pF)	132.1
Inductance of transmitting coil (μH)	51.275
Capacitance of transmitting coil (pF)	4.5499
Inductance of receiving coil (μH)	51.275
Capacitance of receiving coil (pF)	4.5499
Inductance of load coil (μH)	1.7661
Capacitance of load coil(pF)	132.1

The measurements are done by a network analyzer so that the frequency responses (both magnitude and phase) can be measured easily and accurately. The driving and load coils are connected to the ports of the network analyzer through SMA cables and connectors. The measured S-parameter is then converted into the system efficiency.

In order to check the validity of the analysis in the preceding sections, several experiments are conducted for various location combinations as shown in Table 3. The experiments for both the highest efficiency and the longest transfer distance are performed. The measured results and simulated results are compared in Fig. 12.

Table 3: Location combinations of four coils

d (cm)	d_{12} (cm)	d_{23} (cm)	d_{34} (cm)
75	10	55	10
80	10	60	10
85	15	60	10
90	15	60	15
200	60	120	20
220	60	140	20
240	60	160	20
250	70	160	20
260	80	160	20

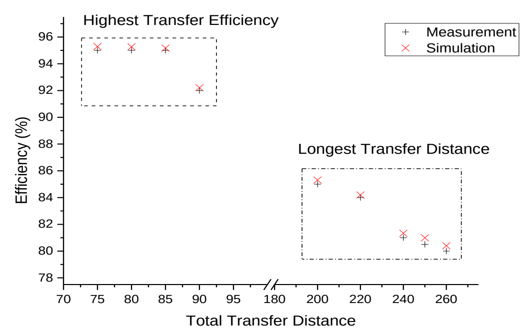

Fig. 12. Comparison of measurements and simulation results.

From Fig. 12, one can observe the highest efficiency is obtained at d_{12} = 10 cm, d_{23} = 55 cm and d_{34} = 10 cm. The highest efficiency is 95.29%. The longest transfer distance is obtained at d_{12} = 80 cm, d_{23}= 160 cm and d_{34} = 20 cm in which the efficiency is slightly higher than 80%. The longest transfer distance d is about 260 cm for a given efficiency of 80%. The measurements agree very well with the simulation results, as shown in Fig. 12.

V. CONCLUSION

Effects of coil locations of the four-coil wireless power transfer (WPT) system via magnetic resonance coupling were studied in-depth here. The location parameters of four coils, including the distance d_{12} between the driving and transmitting coils, the distance d_{23} between the transmitting and receiving coils, and the distance d_{34} between the receiving and load coils, have been used as design variables. It was found that all these three location parameters have impact on the efficiency, the resonant frequency and the bandwidth of the WPT system via magnetic resonance coupling.

The operation of the WPT system via magnetic resonance coupling can be divided into three regions in terms of the distance between each pair of two adjacent coils: over coupling, strong coupling and under coupling. Different operating states can be achieved by adjusting locations of four coils.

The distances d_{12}, d_{23} and d_{34} have different kinds of impact on the efficiency of the WPT system via magnetic resonance coupling. The distance d_{34} has more significant impact on the efficiency than the distance d_{12}. Interestingly, the distance d_{12} has a wide range of the strong coupling state. The efficiency does not change much along with variation of d_{12} in the strong coupling state. The distance d_{23} has also a wide range of the strong coupling state. However, it has strong impact on the bandwidth and the resonant frequency of the WPT system via magnetic resonance coupling. Finally, design guidelines for optimal coil locations have been presented for the WPT system, to which the highest transfer efficiency or the longest transfer distance can be achieved.

ACKNOWLEDGMENT

This work was supported in part by the National Science Foundation of China under Grants 61331007, 61411136003, the Zhejiang Provincial Natural Science Foundation of China under grant LZ14F040001, and the CAST Foundation under Grant CAST201241 and Shenzhen Special Funds for the Development of Strategic Emerging Industries under Grant JCYJ20130401160028789.

REFERENCES

[1] A. P. Sample and J. R. Smith, "Experimental results with two wireless power transfer systems," *in Proc. IEEE RWS*, pp. 16-18, Jan. 2009.

[2] Z. Popovic, E. A. Falkenstein, D. Costinett, and R. Zane, "Low-power far-field wireless powering for wireless sensors," *Proc. IEEE*, vol. 101, no. 6, pp. 1397-1409, June 2013.

[3] B. Strassner and K. Chang, "Microwave power transmission: historical milestones and system components," *Proc. IEEE*, vol. 101, no. 6, pp. 1379-1396, June 2013.

[4] S. Y. Hui, "Planar wireless charging technology for portable electronic products and Qi," *Proc. IEEE*, vol. 101, no. 6, pp. 1290-1301, June 2013.

[5] A. Kurs, A. Karalis, R. Moffatt, J. D. Joannopoulos, P. Fisher, and M. Soljačić, "Wireless power transfer via strongly coupled magnetic resonances," *Science*, vol. 317, pp. 83-86, July 2007.

[6] J. Garnica, R. A. Chinga, and J. S. Lin, "Wireless power transmission: from far field to near field," *Proc. IEEE*, vol. 101, no. 6, pp. 1321-1331, June 2013.

[7] D. Ahn and S. Hong, "A study on magnetic field repeater in wireless power transfer," *IEEE Trans. Industrial Electronics*, vol. 60, no. 1, pp. 360-371, Jan. 2013.

[8] W. X. Zhong, C. K. Lee, and S. Y. R. Hui, "General analysis on the use of Tesla's resonators in Domino forms for wireless power transfer," *IEEE Trans. Industrial Electronics*, vol. 60, no. 1, pp. 261-270, Jan. 2013.

[9] E. M. Thomas, J. D. Heebl, C. Pfeiffer, and A. Grbic, "A power link study of wireless non-radiative power transfer systems using resonant shielded loops," *IEEE Trans. Circuits and Systems I: Regular Papers*, vol. 59, no. 9, pp. 2125-2136, Sept. 2012.

[10] C. K. Lee, W. X. Zhong, and S. Y. R. Hui, "Effects of magnetic coupling of nonadjacent resonators on wireless power Domino-resonator systems," *IEEE Trans. Power Electronics*, vol. 27, no. 4, pp. 1905-1916, Apr. 2012.

[11] A. P. Sample, D. A. Meyer, and J. R. Smith, "Analysis, experimental results, and range adaptation of magnetically coupled resonators for wireless power transfer," *IEEE Trans. Industrial Electronics*, vol. 58, no. 2, pp. 544-554, Feb. 2011.

[12] C.-J. Chen, T.-H. Chu, C.-L. Lin, and Z.-C. Jou, "A study of loosely coupled coils for wireless power transfer," *IEEE Trans. Circuits and Systems II: Express Briefs*, vol. 57, no. 7, pp. 536-540, July 2010.

[13] A. Christ, M. Douglas, J. Nadakuduti, and N. Kuster, "Assessing human exposure to electromagnetic fields from wireless power transmission systems," *Proc. IEEE*, vol. 101, no. 6, pp. 1482-1493, June 2013.

[14] W. Q. Niu, J. X. Chu, W. Gu, and A. D. Shen, "Exact analysis of frequency splitting phenomena of contactless power transfer systems," *IEEE Trans. Circuits and Systems I: Regular Papers*, vol. 60, no. 6, pp. 1670-1677, June 2013.

[15] A. P. Sample, B. H. Waters, S. T. Wisdom, and J. R. Smith, "Enabling seamless wireless power delivery in dynamic environments," *Proc. IEEE*, vol. 101, no. 6, pp. 1343-1358, June 2013.

[16] T. C. Beh, M. Kato, T. Imura, S. Oh, and Y. Hori, "Automated impedance matching system for robust wireless power transfer via magnetic resonance coupling," *IEEE Trans. Industrial Electronics*, vol. 60, no. 9, pp. 3689-3698, Sept. 2013.

[17] W. X. Zhong, C. K. Lee, and S. Y. R. Hui, "Wireless power Domino-resonator systems with non-coaxial axes and circular structures," *IEEE Trans. Power Electronics*, vol. 27, no. 11, pp. 4750-4762, Nov. 2012.

[18] D. Ahn and S. Hong, "Effect of coupling between multiple transmitters or multiple receivers on

wireless power transfer," *IEEE Trans. Power Electronics*, vol. 60, no. 7, pp. 2602-2613, July 2013.

[19] S. Cheon, Y. H. Kim, S. Y. Kang, M. L. Lee, J. M. Lee, and T. Zyung, "Circuit-model-based analysis of a wireless energy-transfer system via coupled magnetic resonances," *IEEE Trans. Industrial Electronics*, vol. 58, no. 7, pp. 2906-2914, July 2011.

[20] C. W. Chang, K. C. Hou, L. J. Shieh, S. H. Hung, and J. C. Chiou, "Wireless powering electronics and spiral coils for implant microsystem toward nanomedicine diagnosis and therapy in free-behavior animal," *Solid-State Electronics*, vol. 77, pp. 93-100, Nov. 2012.

[21] K. Abdelnour, A. Stinchcombe, M. Porfiri, J. Zhang, and S. Childress, "Wireless powering of ionic polymer metal composites toward hovering micro swimmers," *IEEE-ASME Trans. Mechatronics*, vol. 17, no. 5, pp. 924-935, Oct. 2012.

[22] S. Hasanzadeh, S. Vaez-Zadeh, and A. H. Isfahani, "Optimization of a contactless power transfer system for electric vehicles," *IEEE Trans. Vehicular Technology*, vol. 61, no. 8, pp. 3566-3573, Oct. 2012.

[23] J. Kim, H. C. Son, D. H. Kim, and Y. J. Park, "Optimal design of a wireless power transfer system with multiple self-resonators for an LED TV," *IEEE Trans. Consumer Electronics*, vol. 58, no. 3, pp. 775-780, Aug. 2012.

[24] J. S. Ho, S. Kim, and A. Poon, "Midfield wireless powering for implantable systems," *Proc. IEEE*, vol. 101, no. 6, pp. 1369-1378, June 2013.

[25] T. S. Li, Z. Han, H. Ogai, K. Sawada, and J. Wang, "A microchip-controlling wireless power transfer system for sensor network," in *2012 Proceedings Of SICE Annual Conference (SICE)*, pp. 337-341, 2012.

[26] H. Hwang, J. Moon, B. Lee, C.-H. Jeong, and S.-W. Kim, "An analysis of magnetic resonance coupling effects on wireless power transfer by coil inductance and placement," *IEEE Trans. Consumer Electronics*, vol. 60, no. 2, pp. 203-209, May 2014.

Xinzhi Shi received the Ph.D. degree in Computer Application and Technology from Wuhan University, Wuhan, China, in 2005.

She is currently an Associate Professor with the School of Electronics and Information, Wuhan University. Her research interests include optoelectronic device design, modeling, and simulation.

Chang Qi received the Ph.D. degree in Electrical Engineering from Wuhan University, Wuhan, China, in 2007.

She is currently an Associate Professor with the Institute of Microelectronics and Information Technology, Wuhan University. Her research interests include optoelectronic device design, modeling, and simulation.

Shuangli Ye received the Ph.D. degree in Physics and Material Sciences from Philipps University, Marburg, Germany, in 2005.

She is currently an Associate Professor with the Institute of Microelectronics and Information Technology, Wuhan University. Her research interests include nano-engineered magnetic thin film and spintronics MEMS for magnetologic application.

Gaofeng Wang received the Ph.D. degree in Electrical Engineering from the University of Wisconsin, Milwaukee, in 1993 and the Ph.D. degree in Scientific Computing from Stanford University, Stanford, California, in 2001.

From 1993 to 1996, he was a Scientist at Tanner Research Inc., Pasadena, CA. From 1996 to 2001, he was a Principal Research and Development Engineer at Synopsys Inc., Mountain View, CA. In the summer of 1999, he served as a Consultant at Bell Laboratories, Murray Hill, NJ. From 2001 to 2003, he was Chief Technology Officer (CTO) at Intpax, Inc., San Jose, CA. From 2004 to 2010, he was CTO at Siargo Inc., Santa Clara, CA. From 2010 to 2013, he was Chief Scientist at Lorentz Solution, Inc., Santa Clara, CA. From 2004 to 2013, he was also a Professor and the Director for the Institute of Microelectronics and Information Technology, Wuhan University, Wuhan, China. He is currently a Distinguished Professor in Electrical Engineering at Hangzhou Dianzi University, Hangzhou, China.

He has over 280 publications and is the holder of over 20 patents. His research interests include computational electromagnetics, integrated circuits, MEMS and sensor technology, wireless power transfer, and electronic design automation.